Seasonal variations in acidogenic fermentation of filter primary sludge

Water Research 242 (2023) 120181

Contents lists available at ScienceDirect

Water Research

journal homepage: www.elsevier.com/locate/watres

Seasonal variations in acidogenic fermentation of filter primary sludge

Elin Ossiansson [a,b,*], Frank Persson [b], Simon Bengtsson [a,c], Michael Cimbritz [d], David J.I. Gustavsson [a,c]

[a] VA SYD, Box 191, SE-20121 Malmö, Sweden
[b] Chalmers University of Technology, Dep. of Architecture and Civil Engineering, SE-412, 96 Gothenburg, Sweden
[c] Sweden Water Research, Scheelevägen 15, SE-22370 Lund, Sweden
[d] Lund University, Dep. of Chemical Engineering, Box 124, SE-221 00 Lund, Sweden

ARTICLE INFO

Keywords:
Rotating belt filter
Primary sludge
Fermentation
Hydrolysis
Carbon source
Volatile fatty acids

ABSTRACT

Primary treatment of municipal wastewater by rotating belt filtration followed by hydrolysis and acidogenic fermentation of the filter primary sludge (FPS) at ambient temperature was studied at pilot-scale during one year. The seasonal variations of volatile fatty acids (VFAs), nutrient release and soluble COD production as well as microbial community assembly were assessed, leading to novel findings for fermentation at ambient temperature. The reproducibility of VFA production performance was first established by operating the two fermentation reactors under the same conditions, showing similar results regarding VFA production and microbial community structure. One year of operation at 5 d retention time (RT) and 16–29 °C resulted in an average VFA yield of 180 ±35 mg COD/g VS_{in} and soluble COD yield of 242±40 mg COD/g VS_{in}. The VFA formation was temperature-dependent, with Θ=1.033±0.005 ($r = r_{20} \cdot \Theta^{(T-20°C)}$). The seasonal variations of the acetic and propionic acid productions were pronounced, whereas the productions of VFAs with longer chains were more stable regardless of temperature. The community structure of the reactor microbiomes was also clearly affected by season and temperature and linked with the production spectrum of VFAs. The ammonium and phosphate releases were stable during the year, leading to a decrease in ratios of soluble COD to NH_4^+-N and PO_4^{3-}-P during winter. The soluble COD yield was 11% and 27% higher at 5 d RT compared to 3 and 2 d RT respectively, but the corresponding volumetric productivities were lower. The dissimilarities between microbiomes in influent FPS and fermenters were significant even at a short RT of 2 d, and increased with longer RT of 3 and 5 d, primarily caused by selection of bacteria within *Bacteroidota* in the fermentation reactors.

1. Introduction

Municipal wastewater treatment requires a sufficient amount of readily biodegradable carbon for denitrification and excess phosphate uptake in biological nutrient removal (BNR) to meet the effluent demands for nitrogen and phosphorus (Volke et al., 2020). Numerous studies have focused on production and use of volatile fatty acids (VFAs; also known as short chain fatty acids), as carbon sources for BNR (Atasoy et al., 2018; Lee et al., 2014). Biologically produced VFAs are suitable carbon sources for both denitrification and biological phosphorus removal (Elefsiniotis and Wareham, 2007). Settler primary sludge (SPS) and waste activated sludge are often available at wastewater treatment plants (WWTPs) as potential substrates for hydrolysis and fermentation to VFAs, and have been used for this purpose (Andreasen et al., 1997; Bouzas et al., 2002; Pitman et al., 1992; Wang et al., 2020). One possibility to increase the amount of biodegradable carbon for BNR is in-line acidogenic fermentation of SPS in the primary settlers (Banister and Pretorius, 1998; Ekholm et al., 2022; Hey et al., 2012; Tykesson et al., 2005), which is relatively easy to implement, but sensitive to variations of wastewater flow. Side-stream fermentation of SPS, where the sludge is fermented in a separate reactor and recycled to a primary settler, is more flexible compared to an in-line process as it allows for controlled dosing of carbon source to the main stream, but it may cause deteriorated settling properties, and odor (Banister and Pretorius, 1998).

Filtration as primary treatment of wastewater results in smaller footprint and potentially higher removal of total suspended solids (TSS) compared to primary settlers (Väänänen et al., 2016). The sludge that is separated in primary filtration has been denoted primary sludge (Christensen et al., 2022), rotating belt filter (RBF) biosolids (Bahreini

* Corresponding author.
E-mail address: elin.ossiansson@vasyd.se (E. Ossiansson).

https://doi.org/10.1016/j.watres.2023.120181
Received 5 April 2023; Received in revised form 1 June 2023; Accepted 6 June 2023
Available online 7 June 2023

et al., 2021), fine sieved fraction (Ghasimi et al., 2016) or cellulosic primary sludge (Conca et al., 2020), but we propose the generic term filter primary sludge (FPS). FPS from an RBF has a total solids (TS) concentration of 4–10% without integrated dewatering (Rusten et al., 2017), which is considerably higher compared to the TS in both SPS (1.0–3.4%) and waste activated sludge (0.6–1.2%) (Ucisik and Henze, 2008). Hence, it is reasonable to expect a high volumetric VFA production with use of FPS for fermentation. Fermentation of FPS and SPS originating from the same wastewater has resulted in similar VFA yields (Brison et al., 2022), suggesting comparable biodegradability of the two substrates. Polymer addition to the wastewater prior to filtration (chemically enhanced filtration) has been observed to increase the TSS removal and the FPS methane potential (Rusten et al., 2017), but has not been applied in previously published studies of FPS fermentation (Bahreini et al., 2021, 2020a; Da Ros et al., 2020), leaving a knowledge gap concerning the potentials of this substrate.

Fermentation of SPS has occasionally been studied at lower temperatures, below 25 °C (Dauknys et al., 2019; Ferreiro and Soto, 2003; Skalsky and Daigger, 1995). Full-scale fermentation of SPS as an inline process at WWTPs has also been applied at ambient temperature in the Nordic countries (Andreasen et al., 1997; Ekholm et al., 2022; Tykesson et al., 2005). However, the link between temperature and fermentation yield has not been thoroughly addressed. The production rate has been shown to be lower for FPS fermentation below 35 °C (Bahreini et al., 2020b), but fermentation at ambient temperature has the advantage of lower energy requirement. Therefore, the seasonal variations in fermentation of sludge are of practical as well as academic interest.

Acidogenic bacteria can be found in raw SPS even without an intentional fermentation process (Lin and Li, 2018; Maspolim et al., 2015). Consequently, batch tests with fermentation have been conducted successfully without inoculum both with SPS (Miron et al., 2000), and with FPS from RBF (Crutchik et al., 2018; Da Ros et al., 2020). The VFA production could, however, be increased by using fermented sludge as inoculum in batch tests with SPS (Banister and Pretorius, 1998), which implies that hydrolytic and acidogenic bacteria were enriched in fermentation reactors. Both the product spectrum, and microbial community structure were found to be comparable in fermentation of SPS and FPS, indicating that the composition of SPS and FPS, consisting mainly of polysaccharides, selected for similar communities (Brison et al., 2022). Bacteria within *Firmicutes* and *Bacteroidota* that are capable of fermenting were found in the sludge from iron-enhanced primary sedimentation, and multiplied during mesophilic semi-continuous fermentation (Lin and Li, 2018). Temperature ranging from 25 to 55 °C has been shown to have a profound impact on microbial community composition, and can be linked to production of specific VFAs (Huang et al., 2021). Furthermore, the microbial community of FPS anaerobic digestion for methane production has been investigated at mesophilic and thermophilic conditions (Ghasimi et al., 2015), but the community assembly in FPS fermentation at ambient temperature is yet to be mapped out.

In this study, we propose a pre-treatment method for municipal wastewater comprising chemically enhanced prefiltration with RBF and acidogenic fermentation of FPS at ambient temperature. A pilot plant with an RBF and two fermentation reactors was operated for one year with the aim to evaluate the seasonal variations in the fermentation of FPS at ambient temperature, as well as the effects of different retention times (RTs). The corresponding microbial communities were characterised in the influent sludge and in the acidogenic fermentation.

2. Material and methods

2.1. Wastewater pre-treatment

The pilot plant (Fig. S1) was situated at Källby municipal WWTP in Lund, Sweden, which has a load of 90 000 population equivalents, and a low industrial load. Wastewater, screened through 6 mm, was pumped into the pilot plant flow proportionally to the WWTP flow but with a minimum of 6 and maximum of 18 m^3/h during the year of operation in this study (July 2020 to July 2021). The average flow was 11±3 m^3/h with TSS: 242±64 mg/L, COD: 528±111 mg/L, total nitrogen: 55.7 ± 9.6, and total phosphorus: 6.7 ± 1.3. The inlet tank contained online measurement of TSS (VisoLid, WTW) to enable online control for polymer addition. A cationic polymer solution of 0.1–0.2% Superfloc 6260 (Kemira Kemi AB) was added in the pipe to the first of two mixed flocculation tanks (0.8 m^3 each). The polymer was dosed at 1.1–2.0 g/m^3, with additional 5–7 g/g TSS, resulting in a total average polymer dose of 3.2 g/m^3. The particular polymer was chosen since it produced high strength flocs. The total flocculation hydraulic RT (HRT) was 9 ± 3 min.

The RBF (SF1000, Salsnes Filter) was operated with a fixed setpoint for water level at 210 mm (July-April) and 240 mm (April-July), with a filter cloth pore size of 350 μm. The integrated dewatering device was excluded, since the TS of the FPS was otherwise too high to be pumped. Removal of TSS and COD in the RBF was 64±10 and 44±9%, respectively.

2.2. Sludge treatment and sampling

The influent sludge tank had a variable working volume of 0.15–0.38 m^3 and RT of 0.3 ± 0.1 d. The two fermentation reactors were placed outdoors, both insulated and mixed at 70 rpm, with a working volume of 1.5 m^3 each. The steel pipes for sludge were equipped with heat tracing and insulation to avoid freezing during winter. Influent and effluent pumping was automatically controlled at 4–6 times/d for each reactor and the pumping volume was set to achieve the desired RT. During the first operational setting, the verification period, both reactors had a set RT of 5 d (Table 1), which resulted in RTs of 4.9 ± 0.4 and 5.0 ± 0.5 d in R1 and R2 respectively. The RT in the first reactor (R1) was kept at 5.0 ± 0.6 d during a whole year to assess the seasonal variations, whereas the second reactor (R2) was set to first 3 d (3.2 ± 0.7 d) and then 2 d (2.2 ± 0.1 d) during the assessment of different RTs. The effluent sludge was pumped to the pilot plant outlet during the time of this study, and therefore not recycled to the wastewater.

Grab samples of sludge were taken twice/week on alternating weekdays from the lower part of the reactors, and from the influent sludge tank. Temperatures were measured instantaneously on site. During a period in December 2020, the fermentation reactors were heated unintentionally and the temperatures were thus not ambient. In February 2021, the pipes were frozen during two weeks (despite heat tracing and insulation). Both these periods are excluded in the results.

Table 1
Retention time in the two pilot-scale reactors for acidogenic fermentation during the different operational periods.

		Jul	Aug	Sept	Oct	Nov	Dec	Jan	Feb	Mar	Apr	May	Jun	Jul
R1	RT (d)	5												
R2	RT (d)	5								3		2		
Periods		Assessment of seasonal variation (R1)												
		Verification period (R1,R2)								Assessment of different RTs (R1,R2)				

Data was also excluded if there was a deviation of RT due to error in pumping or flow measurement.

2.3. Chemical analyses

TS and volatile solids (VS) were analysed after 24 h at 105 °C, and after 2 h at 550 °C. COD and ammonium-nitrogen were measured with spectrophotometric cuvettes (Hach LCK114 and LCK304). Samples for analysis of soluble COD and specific VFAs were first centrifuged (5000 rpm, 5 min) and subsequently filtered through glass-fiber filters with pore size 20 μm (Munktell MGA No:110 116) and 0.45 μm syringe filters (Sartorious Minisart RC 25). For pH measurements, a pH electrode was used (Metrohm/Xylem). Samples for analysis of ammonium nitrogen and phosphate phosphorus were first filtered through 1.6 μm glass fiber filters (Whatman, No 1820–055). Phosphate phosphorus and total phosphorus were analysed in 20 mL samples with spectrophotometry (PerkinElmer Lambda 35) after acidification with 4 M H_2SO_4. Kjeldahl nitrogen in sludge samples was measured according to SS-EN 16,169:2012 with analyser unit Kjeltec 8420 and compass software 2.2 (Foss Analytics). VFAs were measured both as acetic acid equivalents (HAc-eq) with 5-point titration according to Ibrahim et al. (2014), and as separate acids with either gas chromatography (GC) or high-performance liquid chromatography (HPLC). The 5-point titration also provided values of total alkalinity.

For the measurement of specific VFAs with GC or HPLC, the same standard solution (Volatile Free Acid Mix, Merck) was used for calibration. Samples for VFA analysis (900 μL) were conserved with 100 μL 10% w/w phosphoric acid. The GC (Agilent 6850) was equipped with a 30 $m \times 0.53$ mm $\times$ 1 μm column (19095F-123E, Agilent). Nitrogen gas was used as carrier, while hydrogen gas was added for flame ionization. The temperature was raised from 80 °C to 120 °C at a rate of 20 °C/min, thereafter from 120 °C to 130 °C at a rate of 6.13 °C/min, whereafter the temperature was kept constant at 130 °C for 5 min. Injection temperature was 180 °C, and detector temperature 260 °C. Injection volume was 1 μL. The HPLC (1269 Infinity II Quaternary System, Agilent) was operated at 60 °C during 60 min with a flow of 0.7 mL/h through the column (InfinityLab Poroshell 120 EC-C18). For each sample, 20 μL was injected and the variable wavelength detector signal at 210 nm was used for quantification with OpenLAB (Agilent). Phosphoric acid (0.1% w/w) was used as carrier solution.

Batch tests for measurement of denitrification rate was conducted with influent and filtered wastewater, as well as filtered wastewater with added fermentate according to the procedure described in the supplementary material.

2.4. Microbial community analysis

Biweekly samples of the influent sludge to the reactors, R1, and R2 over the entire operational period starting from June 2020 (in total 98 samples) were subjected to amplicon sequencing. Experimental procedures are described in detail in the supplementary material. In brief, DNA was extracted and the V4 region of the 16S rRNA gene was amplified by polymerase chain reaction (PCR). After purification, quality control and measurement of DNA concentrations, the pooled PCR products were sequenced on a MiSeq (Illumina). Processing of the obtained raw sequence reads and generation of count tables with amplicon sequence variants (ASVs) were carried out using DADA2 v1.16 (Callahan et al., 2016) and VSEARCH (Rognes et al., 2016) in parallel. A consensus count table from the two pipelines were generated using qdiv (Modin et al., 2020). Taxonomy was assigned with SINTAX (Edgar, 2016) using the Midas 4.8.1 database (Dueholm et al., 2022).

The bioinformatics and diversity calculations were carried out in qdiv (Modin et al., 2020). The dataset was rarefied by subsampling each sample to 35 957 reads. Alpha and beta diversity was calculated using the Hill number framework (see the supplementary material for details). Dissimilarities between samples were visualized using principal coordinate analysis (PCoA). To determine the dissimilarity caused by compositional turnover between samples and assess the roles of deterministic and stochastic factors for microbial community assembly, the Raup-Crick null model (Chase et al., 2011; Raup and Crick, 1979) was used, adapted for Hill-based dissimilarities in qdiv (Modin et al., 2020). Redundancy analysis (RDA) of the top 25 genera in R1 (having constant RT) and selected environmental data was carried out in the R-package vegan v2.6.4 (Oksanen et al., 2022) using the rda function, after doing a Hellinger transformation of the community abundances using the decostand function. For more details on bioinformatics, see the supplementary material. Raw sequence reads are deposited at the Sequence Read Archive, NCBI, Bioproject: PRJNA945084.

2.5. Calculations

Given its 0.3 d average RT, the influent sludge tank was considered as part of the total process volume. The soluble COD and VFA yields (Y) were thus calculated based on the difference between reactor concentrations and influent wastewater concentrations. As the influent wastewater concentrations were negligible compared to the reactor concentrations, the yields were calculated according to Eq. (1), where VS_{in} is the mean value of influent VS during a period of two weeks.

$$Y = \frac{[Reactor]}{VS_{in}} \quad (1)$$

In models for BNR, all conversion rates can be multiplied by a temperature-dependency factor, often in the form of Eq. (2), where r is the reaction rate and T is the temperature in °C (Rieger et al., 2013). Since the RT was kept constant, Eq. (2) could be simplified to Eq. (3), where the Y is the observed yield during the experimental period and Y_{20} is the observed yield at 20 °C. The fitting of the temperature dependency constant Θ was carried out in Origin (OriginLab) using Levenberg Marquardt iteration.

$$r = r_{20} \cdot \theta^{(T-20°C)} \quad (2)$$

$$Y = Y_{20} \cdot \theta^{(T-20°C)} \quad (3)$$

Two-sided student *t*-test conducted for paired data, as well as the calculations of standard deviations were made in Excel 2019 (Microsoft).

3. Results

3.1. Acidogenic fermentation was highly reproducible

Filtration of municipal wastewater with RBF resulted in a sludge with 4.5 ± 0.6% TS and 87.5 ± 4.4% VS of TS with an average concentration of 57 200±13 400 mg COD/L (Table 2). The two reactors (R1 and R2) for acidogenic fermentation of FPS were first operated as duplicates with the same RT of 5 d, with similar results. The VFA concentrations were 8 070±1 360 and 8 060±1 420 mg COD/L in R1 and R2 respectively (Fig. 1). Likewise, the mean VFA distributions were very similar in both reactors; 27±1% acetic acid (HAc), 42±2% propionic acid (HPr), 3 ± 0% isovaleric acid (Iso-Hbu), 14±1% butyric acid (Hbu), 5 ± 1% Iso valeric acid (Iso-Hval), 9 ± 1% valeric acid (Hval), expressed as% of VFA-COD, (n = 14 for each reactor). The difference in mean values for 13 process parameters were 0.4–4.5% between the reactors. For 10 parameters, no differences were observed (p>0.05), while significant deviations were found for three parameters with minor differences (SM, Table S1).

Table 2
Mean values ± standard deviations for process variables in the influent sludge tank, and the acidogenic fermentation reactor R1 during one year of operation at ambient temperature and 5 d RT.

Parameter	Unit	No.	Influent sludge tank	R1, RT 5 d
Temperature	°C	75	21.1 ± 3.1	22.2 ± 3.6
pH		78	5.9 ± 0.3	5.2 ± 0.1
Total solids	%	78	4.5 ± 0.6	3.8 ± 0.5
Volatile solids	% of TS	78	88±4	87±2
Ammonium nitrogen	mg/L	78	126±52	438±72
Kjeldahl nitrogen	mg/kg TS	76	31 100±5 100	35 500±5 100
Phosphate phosphorus	mg/L	78	69±27	157±29
Total phosphorus	mg/L	82	329±58	310±50
Total alkalinity		74	1 480±380	3 350±280
Chemical oxygen demand	mg COD/L	82	57 200±13 400	61 800±16 200
Soluble chemical oxygen demand	mg COD/L	58	3 340±1 350	9 480±1 260
Volatile fatty acids	mg HAc-eq/L	78	1 220±500	4 260±590
Volatile fatty acids	mg COD/L	48	2 080±860	7 160±1 410
COD to VS ratio	mg COD/g VS	68	1 470±350	1 920±680
COD solubilisation	% of COD	51	6 ± 3	16±5
Nitrogen solubilisation	% of N	76	9 ± 4	33±8
Phosphorous solubilisation	% of P	69	22±8	51±6
Soluble COD to NH_4^+-N ratio	g COD/g NH_4^+-N	59	30±14	23±4
Soluble COD to PO_4^{3-}-P ratio	g COD/g PO_4^{3-}-P	59	54±32	63±15
VFA to soluble COD ratio	%	41	65±21	77±18
VFA to VFA-eq	g COD/g HAc-eq	47	1.8 ± 0.6	1.7 ± 0.2
Organic loading rate	kg VS/ (m^3, d)	76		8.0 ± 1.4
Soluble COD yield	mg COD/g VS_{in}	57		242±40
Soluble COD production	g COD/ (m^3, d)	57		1 880±280
VFA yield	mg HAc-eq/g VS_{in}	73		108±16
VFA production	g HAc-eq/ (m^3, d)	78		852±118
VFA-COD yield	mg COD/g VS_{in}	47		180±35
VFA-COD production	g COD/ (m^3, d)	47		1 430±280

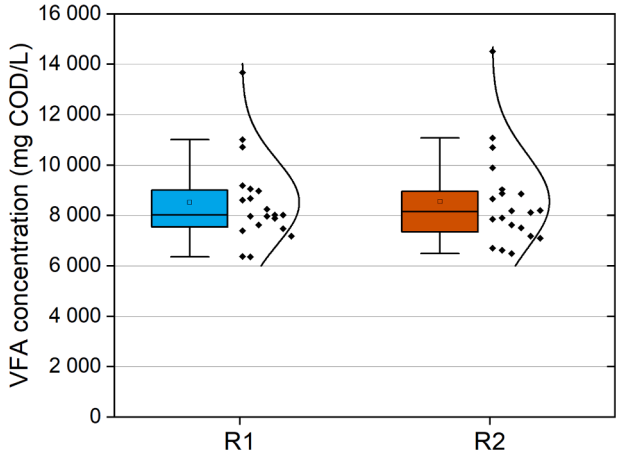

Fig. 1. VFA concentrations in reactors R1 and R2 during the verification period of parallel operation at 5 d RT. Boxes mark 25 to 75% percentiles with a line for 50% and a marker for mean value. The error bars mark the standard deviations.

3.2. Considerable seasonal variations in fermentation at ambient temperature

The temperature ranged from 16 to 29 °C during one year of operation of R1 at the RT of 5 d. The observed soluble COD yield was 242 ±40 mg COD/g VS_{in}, of which VFAs constituted 180±35 mg COD/g VS_{in}, corresponding to 108±16 mg HAc-eq/g VS_{in} (Eq. (1), Table 2). A clear seasonal dependency can be seen for soluble COD and VFA concentrations (Fig. S2a) and observed VFA yield (Fig. 2a) with a peak in September, and minimum in March. The VFA yield deviated, however, from the temperature curve during January and May-June (Fig. 2a). Curve fitting of the observed VFA-COD yield versus the temperature (Eq. (3), Fig. 2b) rendered a yield at 20 °C, Y_{20}, of 172±4 mg COD/g VS_{in}, and θ of 1.033±0.005 (R^2=0.55). Measurements of VFA with titration, which were carried out in parallel and at higher frequency, gave a Y_{20} of 103 mg HAc-eq/ g VS_{in} and a slightly lower value for θ of 1.029±0.004 at R^2=0.56 (Fig. S2b).

The temperature dependencies of ammonium and phosphate were weak. Due to the strong temperature dependence for the VFA formation, the ratios of soluble COD to nutrients were higher during summer than during winter (Fig. 3). The soluble COD to NH_4^+-N ratio was ranging

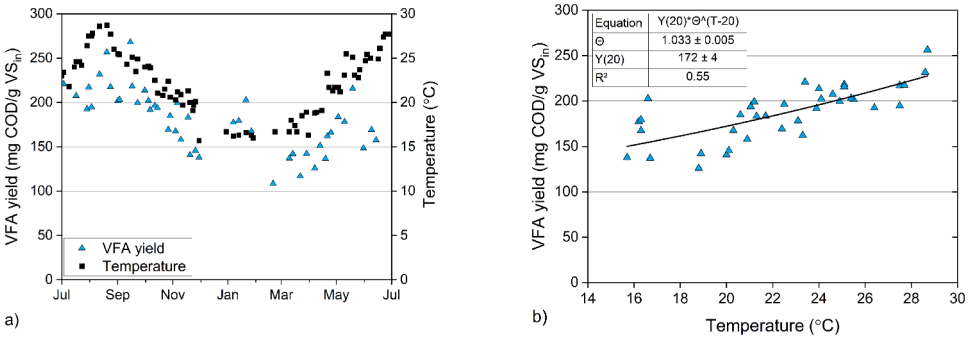

Fig. 2. Seasonal variations in reactor R1 for acidogenic fermentation of RBF sludge during one year of operation with 5 d RT a) VFA yield and temperature. b) Curve fitting of the VFA yield versus temperature.

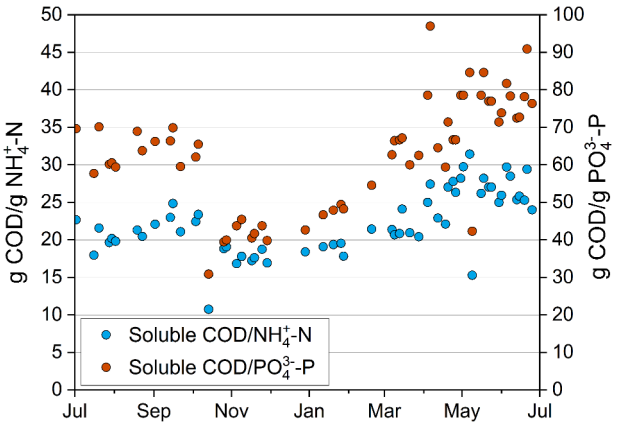

Fig. 3. Soluble COD to nutrient ratios in R1 during one year of acidogenic fermentation at 5 d RT.

from 17 to 20 g COD/g NH_4^+-N during winter to 20–30 g COD/g NH_4^+-N during summer. A similar temperature effect was observed for the soluble COD to PO_4^{3-} ratio, which was 20–25 g COD/g PO_4^{3-} -P during winter, and rose to 30–45 g COD/g PO_4^{3-}-P during summer. The maximum denitrification rate for filtered wastewater was increased from 6.3 to 9.0 mg NO_3^--N eq/ (g VSS, h) with addition of fermentate (Fig. S4).

HPr was the dominating VFA on COD basis followed by HAc, and they both displayed a clear seasonal variation (Fig. 4a, b). The yields of HBu, Iso-HBu, HVal and Iso-HVal were more stable throughout the year (Fig. 4a, b). The temperature correlations for the observed yields of HAc and HPr were Y_{20}=42±1, Θ=1.042±0.007, (R^2=0.48); and Y_{20}=63±2, Θ=1.054±0.007, (R^2=0.59) respectively (Fig. 4b). Consequently, the fraction of HPr increased with higher temperature (Fig. S3). Furthermore, the fraction of HBu was unusually high in March, after the period of operational problems (Fig. S3).

3.3. Both carbon source production and quality were affected by retention time (RT)

During March-June, when the two reactors R1 and R2 were operated at different RTs, temperatures in both reactors were rising, from 16 to 28 °C. There was a statistically significant difference of 11% in the observed soluble COD yield already during period 1 from March to mid-May when R1 was operated at 5 d RT and R2 at 3 d RT, with 258±43 and 230±27 mg COD/g VS_{in} in R1 and R2, respectively (Table 3). The volumetric SCOD production was, on the other hand, 50% lower at the longer RT; 2 000±200 compared to 3 000±200 g SCOD/ (m^3, d) in R1 and R2, respectively.

When the RT was lowered to 2 d in R2, during period 2 from mid-May to mid-June, the difference in SCOD yield increased to 27% with 263±36 and 191±33 mg COD/g VS_{in} in R1 and R2, respectively. The volumetric SCOD production was 78% lower in R1 than R2; 1 800±200 compared to 3 300±400 g COD/ (m^3, d) (Table 3). Meanwhile, the observed HAc-eq yield was less affected by RT than the volumetric SCOD production: 34% lower at 3 d RT and 48% lower at 2 d RT compared to 5 d RT.

The ratios of SCOD to NH_4^+-N (Table 3) were similar during the first period, which suggests that the fraction of soluble COD derived from hydrolysis of proteins were comparable at RT of 5 and 3 d; 25 g SCOD/g NH_4^+-N. During period 2, the difference was minor, resulting in ratios of 26±2 and 23±3 g COD/g NH_4^+-N in R1 and R2, respectively. The ratios of soluble COD to PO_4^{3-}-P (Table 3) displayed a small but statistically significant difference during the first period with 70±13 and 64±14 g COD/g PO_4^{3-}-P in R1 and R2. The difference grew during period 2, with 77±4. and 65±6 g COD/g PO_4^{3-}-P.

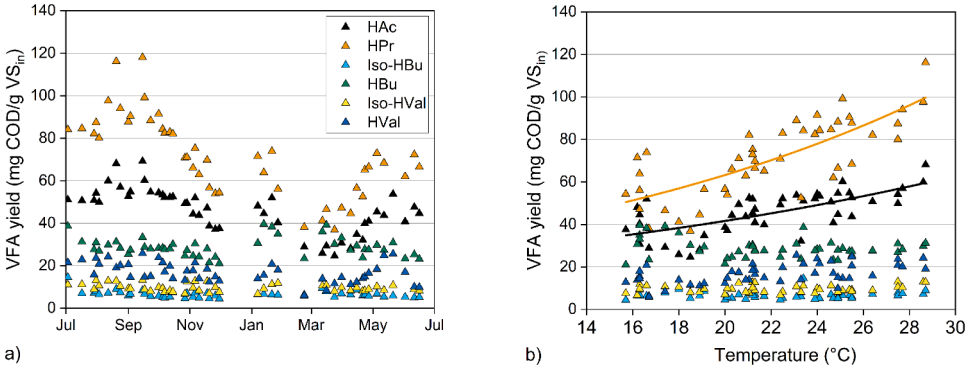

Fig. 4. Yields of VFAs vs (a) time (b) temperature, in R1 during one year of operation at 5 d RT and ambient temperature.

Table 3
Yields of SCOD and VFAs as well as SCOD to nutrient ratios for fermentation of RBF sludge at ambient temperature in reactors R1 and R2 with different RTs, presented as mean± standard deviations.

Parameter	Unit	Period 1			Period 2		
		No. of samples	R1 RT 5 d	R2 RT 3 d	No. of samples	R1 RT 5 d	R2 RT 2 d
Soluble COD yield	mg COD/g VS_{in}	14	258±43	230±27	7	263±36	191±33
Soluble COD production	mg COD/ (m^3, d)	14	2 000±200	3 000±200	7	1 800±200	3 300±400
VFA-COD yield	mg COD/g VS_{in}	10	153±24	123±33	3	189±29	126±420
VFA-COD production	mg COD/ (m^3, d)	10	1 200±100	1 600±300	3	1 300±200	1 900± 200
VFA-eq yield	mg HAc-eq/g VS_{in}	16	100±14	87±9	8	123±3	87±9
VFA-eq production	mg HAc-eq/ (m^3, d)	16	770±60	1 100±50	8	830±40	1 500± 200
Soluble COD to NH_4-N ratio	COD/NH_4^+-N	14	25±4	25±6	8	26±2	23±3
Soluble COD to PO_4-P ratio	COD/PO_4^{3-}-P	14	70±13	64±14	8	77±4	65±6

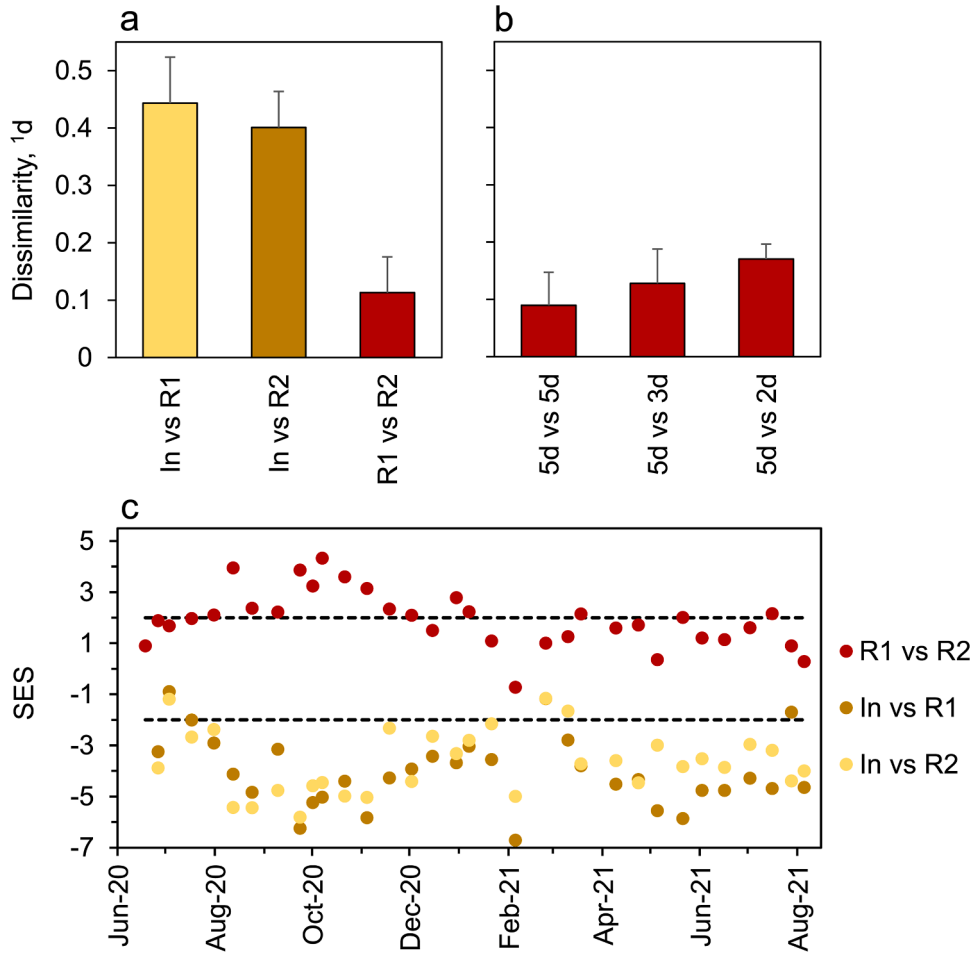

Fig. 5. Pairwise dissimilarities ($q = 1$) between the microbiomes in the influent FPS (In) and the biomass in R1 and R2. a) Comparisons between In, R1 and R2 over the entire period of 13 months. b) Comparisons between R1 (operated at 5 d RT) and R2 (operated at 5, 3, and 2 d RT). c) Null modeling using Raup-Crick displayed as the standard effect size (SES) over time. The hatched horizontal lines designate two standard deviations from null.

3.4. The microbiomes in the fermentation reactors were distinctly different from the influent filter primary sludge

The diversity within samples (alpha diversity) was lower in the reactor microbiomes than in the reactor influent FPS ($p<0.001$) considering both species richness (number of ASVs, ^{0}D) and when taking the relative abundance of ASVs into account (^{1}D) (Fig. S5).

When comparing the microbial community structure between the reactor and the influent FPS microbiomes (beta diversity), as pairwise dissimilarities over 13 months of operation (Fig. 5a), it was clear that the reactors harboured microorganisms with a community structure distinctly different from the influent FPS. It was also evident that the two reactors, when operated at the same RT, had similar microbiomes (Fig. 5b), which is in line with the similar VFA production from the two reactors during this period (Fig. 1). The patterns of a clear separation of the microbiomes in reactors and influent, as well as the minor differences between the replicate reactors, was confirmed by PCoA ordination (Fig. S6). When decreasing the RT to 3 and 2 d of R2, while keeping it at 5 d in R1, differences between microbiomes in the two reactors increased (Fig. 5b), as did the yield of VFA (Table 3).

The null model analysis showed that the microbial community composition in the reactors were more dissimilar to the influent sludge than could be explained by chance (Fig. 5c). The analysis also showed that the composition in the parallel reactors were more similar to each other than could be expected by chance, especially when operated at the same RT of five days during the verification period. But even at shorter RT, the microbiomes in R2 were distinctly different from the influent (Fig. 5c).

3.5. Bacteria within Bacteroidota were highly enriched in the reactors

Seven phyla had an average relative abundance exceeding 1% in either the reactors or the influent FPS. In the influent, *Firmicutes* and *Proteobacteria* were the largest phyla accounting for 36% and 34% of the microbiomes, with smaller contributions of *Bacteroidota* (13%), *Actinobacteriota* (5.3%) and *Camplylobacteriota* (5.0%) (Fig. S7). In the reactors, bacteria within *Bacteroidota* were clearly enriched with relative abundances of 47% and 44% in R1 and R2 respectively, at the expense of bacteria within the other phyla. Especially bacteria within *Proteobacteria* had profoundly lower relative abundances of 14% in R1 and 15% in R2. Within *Bacteroidota*, a number of genera were enriched in the reactors, for instance *Prevotella, Prevotella 9*, and the Midas genera 47,113 and 51,577 within *Prevotellaceae* (Dueholm et al., 2022) as well as U29-B03 within *Rikenellaceae* (Fig. 6). The reactor conditions explained 68% of the variation of the abundant genera in the R1 microbiome, as revealed by RDA (Fig. S8). Among the genera within *Prevotellaceae* and *Rikenellaceae*, various associations with reactor conditions were observed, with *Prevotella 9* correlating with the concentrations of HBu, U29-B03 with Iso-HBu, and Midas genus 47,113 and *Prevotellaceae* SV5557 with HAc.

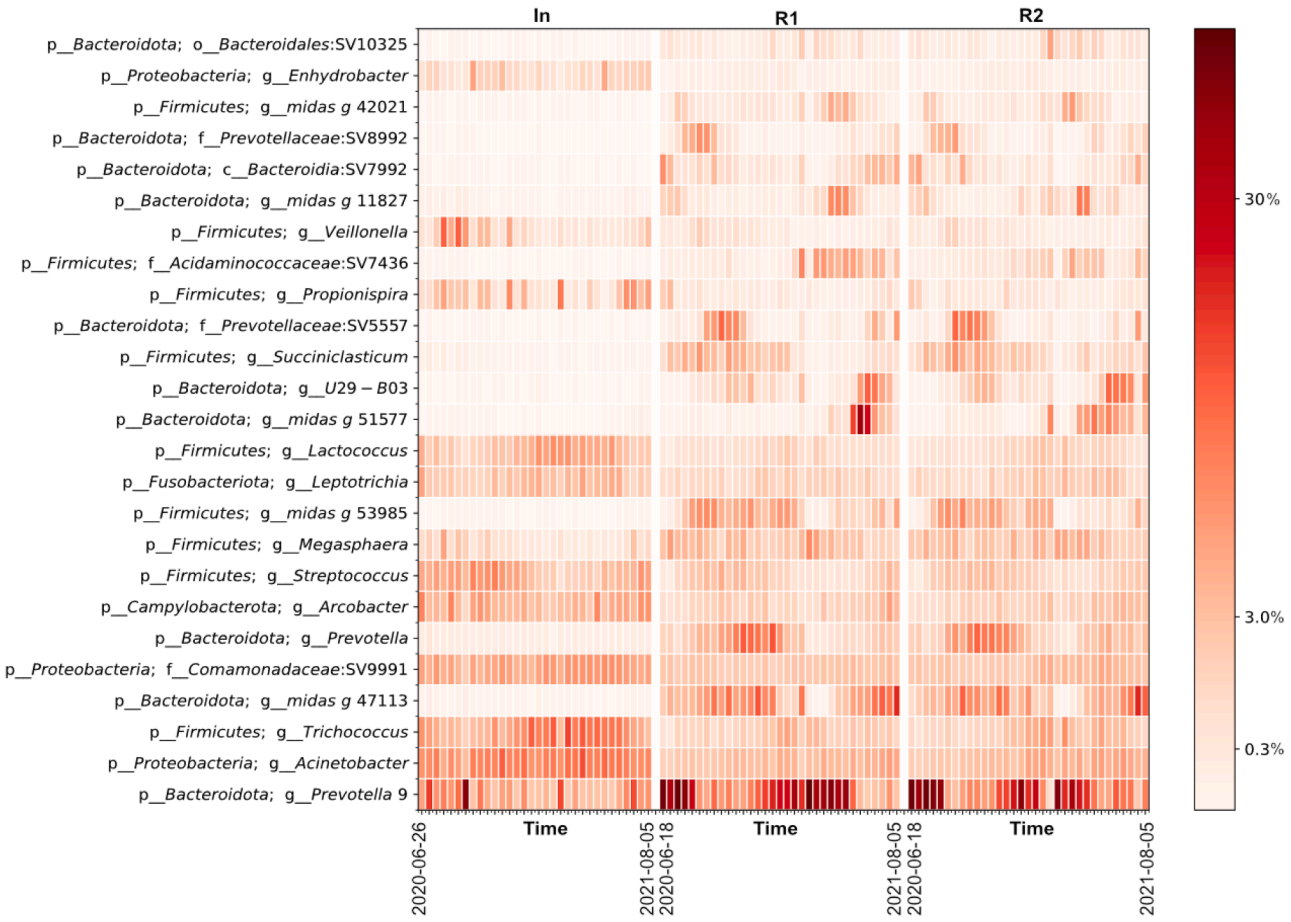

Fig. 6. Heatmap showing the 25 most abundant genera in the influent FPS (In) and the biomass in R1 and R2.

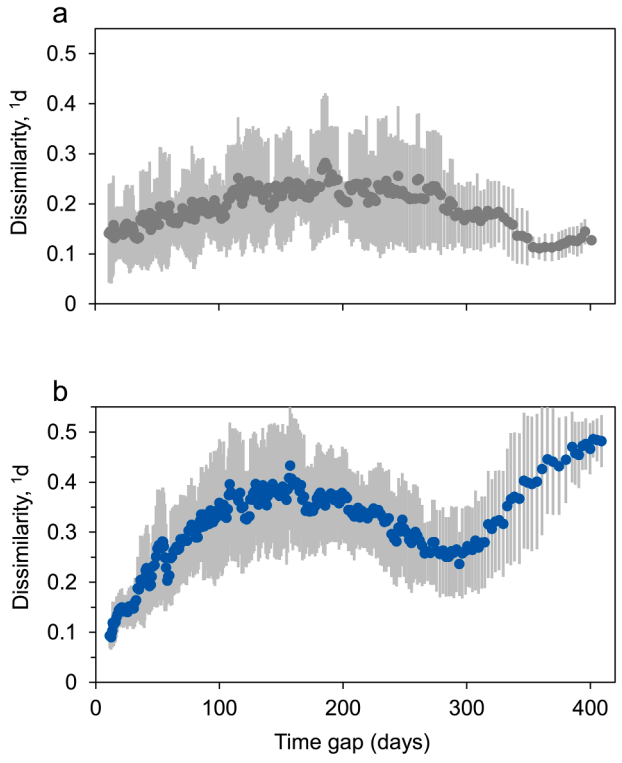

Fig. 7. Dissimilarity ($q = 1$) of microbiomes as a function of time gap between sampling occasions. a) Influent FPS (In) and b) R1. The data points (dark gray or blue) represent averages and the error bars (light gray) standard deviation.

3.6. Changes over time in community structure

Over time, the microbiomes changed at similar rates of about 0.01 d^{-1} suggesting a rather stable succession in the reactors as well as the influent FPS (Fig. S9). However, a few peaks in rate of change were observed, for instance around February 2021 when the temperature fluctuated considerably and feeding of sludge to the reactors was temporarily halted. Community dissimilarity at various time gaps (Fig. 7) indicated seasonal patterns with a maximum dissimilarity at 5 (R1) and 6 months (FPS) time gap, and a secondary minimum at 10 (R1) and 12 months (FPS).

4. Discussion

4.1. Carbon source production

The results in this study support the reproducibility of FPS fermentation, with similar microbial community structure in the two pilot-scale reactors producing VFA and other chemical components in an equal manner (Figs. 1 & 5, Table S1). A few operational disturbances, such as failure of pumps and unintentional heating, did not have any long-term effects on the microbial community structure and process performance, suggesting process robustness. Reproducibility of duplicate lab-scale reactors with influent from the same batch of primary sludge was observed already by Eastman and Fergusson (1981). Reproducibility at pilot-scale with its larger variation in environmental conditions, as shown in this study, is promising for application in full-scale.

The soluble COD yield of 242±40 mg COD/g VS_{in} during one year at 5.3 d RT at 16–29 °C (including the sludge tank) is comparable to the yield of 267 mg COD/g VS during fermentation at 25 °C and 4 d RT

(Bahreini et al., 2020b). Furthermore, the VFA yield of 180±35 mg COD/g VS is comparable to 154 mg COD/g VS from FPS at 6 d RT and 37 °C (Da Ros et al., 2020) and 162±13 mg COD/g VS for fermentation at 4 d RT and 37 °C (Crutchik et al., 2018), although the temperature was varying and lower in this study. In conclusion, the FPS substrate, and fermentation conditions at ambient temperature in this study resulted in similar yields, compared with previous findings.

The RT had clear effect on the soluble COD and VFA, with considerably higher yields at 5 days than 2 or 3 days (Table 3). This supports previous findings of soluble COD production from FPS that increased from 173 to 267 mg COD/g VS when increasing RT from 2 to 4 d at 25 °C (Bahreini et al., 2020b). Since an RT of 5 d produced a fermentate with higher VFA/PO_4^{3-}-P compared to at shorter RT, longer RT would be more favourable for application of the fermentate as carbon source for enhanced biological phosphorus removal.

4.2. Seasonal variations

The seasonal variation in temperature (16–29 °C) had profound effect on the production of VFA (Fig. 4). Accordingly, the community dissimilarity as a function of time gap (Fig. 7) indicated that the microbial community in the fermenters also varied seasonally. The temperature dependency constant for VFA production was θ=1.033. The only previous FPS study found at this point for comparable temperatures of 25 and 35 °C (Bahreini et al., 2020b), report VFA yields that can be used to calculate temperature dependency of θ~1.04 at an RT of 4 d Although the studies are not directly comparable, the similar θ-values between the studies suggest a general response of acidogenic fermentation of FPS sludge to temperature variation.

Among the VFA components, the production of HAc and HPr was higher during the warmer months, while the production of the other VFAs was rather stable over the year. HAc and HPr have been shown to be the major products from fermentation of both SPS and FPS (Brison et al., 2022; Huang et al., 2021), but the results of temperature impact on the VFA distribution in previous studies have not been consistent. Increasing temperature during fermentation of SPS has shown profound impact on the fractions of produced HAc and HPr, but in various directions, while the fraction of larger VFAs have been either rather unaffected or increased at increasing temperatures (Cokgor et al., 2009; Ferreiro and Soto, 2003; Huang et al., 2021). The VFA composition is worth considering, since HAc and HBu have been found to be preferred substrates to HPr for denitrifying bacteria (Elefsiniotis and Wareham, 2007), meaning that the fermentate in this case might be a more appealing substrate for denitrification when it is produced at lower fermentation temperature. Although the soluble COD to ammonium ratio was lower during winter (17–20 g COD/g NH_4^+-N), it was still high compared to the theoretical requirement of 3.74 g COD/g N for denitrification with HAc (Chiu and Chung, 2003). HPr is, on the other hand, an attractive substrate for EBPR (Moser-Engeler et al., 1998).

The stable concentrations of ammonium and phosphate implies that the degradation of proteins was rather unchanged, and that degradation of carbohydrates was responsible for the seasonal variation of VFA production. Degradation of fat is inhibited during acidic conditions, since methanogenic bacteria are needed for uptake of hydrogen in order to create a thermodynamically favourable environment for lipid conversion (van Lier et al., 2020). VFAs with longer chains can be produced from proteins via the Stickland reaction (Ramsay and Pullammanappallil, 2001). The stable concentrations of both ammonium and phosphate over time is consequently in line with the lack of seasonal variation for HBu, Iso-HBu, HVal and Iso-HVal. Fermentation of sucrose with both HAc and HPr as products is more favourable energetically compared to fermentation to only HBu, or HAc (van Lier et al., 2020), which is presumably the reason for the production of these two VFAs as the dominant pathway exhibiting the same temporal trend.

At a full-scale plant, the practical and economic advantages of operating a process at ambient temperature can be weighty, despite the lower reaction rate. This study brings new and useful insights to the seasonal variations of fermentation at ambient and transient temperature, which are likely similar to the existing fermentation of SPS running at numerous WWTPs. Since the cellulose content is higher in FPS compared to SPS (Ahmed et al., 2019), the seasonal variation in the production of HAc and HPr is likely to be less pronounced, but may occur also in full-scale fermentation of SPS.

4.3. Microbial community structure

The observed separation in microbial community structure between the influent FPS and the reactor biomass (Fig. 5a, Fig. S6) was caused by both differences in species richness (Fig. S1) and compositional differences (species turnover), as revealed by the null-models (Chase et al., 2011; Modin et al., 2020). The null-model results (Fig. 5c) furthermore suggests that deterministic forces, such as reactor conditions and species interactions, were vital for shaping the reactor microbiomes and that stochastic immigration, birth, and death, were of limited importance (Chase and Myers, 2011; Zhou, 2017). In various wastewater treatment reactors and anaerobic digestors, deterministic forces have been assigned important roles for shaping the microbiomes (Ali et al., 2019; de Celis et al., 2022; Liébana et al., 2019; Vanwonterghem et al., 2014). However, the investigated reactors have been operated at considerably longer retention times, which promotes deterministic species selection (Ali et al. 2019). Our results indicate that even a few days of RT would suffice for deterministic selection of reactor microbiomes, at least for fermentation reactors. The results also put the many findings in fermentation reactors of different microbial communities at various environmental conditions (e.g. Brison et al., 2022; Maspolim et al., 2015; Yuan et al., 2016) in context.

In the reactor microbiomes, bacteria within *Bacteroidota* were enriched, while *Proteobacteria* were strongly reduced in abundance (Fig. 7& S7). It has been suggested that *Proteobacteria* generally harbours bacteria with low activity at anaerobic conditions, why their presence in fermentation reactors is mainly a factor of immigration, rather than growth (Brison et al., 2022; Mei et al., 2016), which fits well with the observations here. The enrichment of bacteria within *Bacteroidota* also confirms previous findings of high abundances of bacteria within this phylum in fermentation reactors (Brison et al., 2022; Esquivel-Elizondo et al., 2017; Huang et al., 2021; Maspolim et al., 2015). Little is known about the physiology of the enriched genera within *Bacteroidota*, mainly belonging to *Prevotellaceae* and *Rikenellaceae* (Dueholm et al., 2022), except that they are likely anaerobic and fermentative, capable of hydrolysing polysaccharides and proteins (Abe et al., 2013; Könönen et al., 2010; Krieg, 2010). Members in *Rikenellaceae* and *Prevotellaceae* are often associated with the gut microbiome but have also been assigned important roles for VFA production in fermentation reactors (Brison et al., 2022; Esquivel-Elizondo et al., 2017). In the gut microbiome, bacteria within *Prevotellaceae* are associated with the fermentation of fiber (Precup and Vodnar, 2019), which may explain its high abundance in fermentation reactors treating FPS containing a particularly high cellulose content (Ahmed et al., 2019). The observation that various genera within *Prevotellaceae* were correlated with different VFA components in the reactor, as indicated by RDA (Fig. S8), furthermore suggests functional variation among the genera, which seems likely as bacteria within *Prevotellaceae* have genes for production of a number of VFA species (Esquivel-Elizondo et al., 2017).

The reactor microbiome showed clear seasonal patterns, most likely driven by the variation in temperature (Fig. 7). For instance, one of the main genera, *Prevotella* 9, was mostly abundant at cold conditions and seemingly linked with HBu production (Fig. S8). Temperature has previously been identified as the key seasonal factor for community succession in activated sludge (de Celis et al., 2022; Griffin and Wells, 2017). Here, the reactor microbiome exhibited more pronounced and somewhat different seasonal patterns than the influent FPS (Fig. 7), probably caused by the sharp temperature gradients in the reactor

(Fig. 3). Altogether, the findings highlight that the fermentation microbiome was largely influenced by the reactor conditions, of which temperature was a main factor, which thereby caused seasonal variation in the spectrum of produced VFAs.

5. Conclusions

- Fermentation of FPS at pilot-scale was reproducible and stable, with insignificant differences in VFA production and microbial community structure between parallel reactors operated at 5 d RT.
- Seasonal variations had considerable influence on the VFA production rate (and thus the observed yield) and the microbial community structure. HAc and HPr formation displayed strong temperature dependencies, while the formation of longer chained VFAs was more stable. The seasonal pattern of VFA production during fermentation at ambient temperature has not been shown before, although it is of importance for subsequent BNR.
- The nutrient solubilisation was less temperature-dependent than the VFA production and COD solubilisation, observed as lower ratios for SCOD/PO_4^{3-}-P and SCOD/NH_4^+-N in the fermentate during winter. Consequently, the carbon source quality for nutrient removal would decrease at lower temperature.
- Lower RT of 2 and 3 d resulted in a higher volumetric productivity and may hence be suitable if there is an existing but restricted volume to be used for fermentation. In a greenfield installation, a longer RT of 5 d (or longer) is preferable to increase the yields of soluble COD and VFA, as well as soluble COD to nutrient ratios.
- The microbial community structure in the fermentation process was to a large extent shaped by process conditions and biotic interaction with preferable enrichment of bacteria within *Bacteroidota* and wash out of bacteria within *Proteobacteria*.

Declaration of Competing Interest

The authors declare the following financial interests/personal relationships which may be considered as potential competing interests:

David Gustavsson, VA SYD reports financial support was provided by Swedish Environmental Protection Agency. David Gustavsson reports financial support was provided by Sweden Water Research. David Gustavsson reports financial support was provided by The Swedish Water & Wastewater Association. Frank Persson reports financial support was provided by Foundation for J Gust Richerts minne.

Acknowledgements

The pilot plant construction was partially funded by the Swedish Environmental Agency through the program City Innovations (NV-02084–18). In addition, the study was funded by VA SYD, Sweden Water Research, the foundation for J. Gust Richerts minne (2021–00753), and by the Swedish Water and Wastewater Association (19–112). The authors would like to acknowledge the laboratory (VA SYD) for their contribution, and the operational personnel at Källby WWTP (VA SYD) as well as the master thesis students Sara Tebini and Sanna Sahlin. The authors would also like to thank Mirjam Victorin and Mats Galbe (Lund University) for introduction to VFA measurement with GC and HPLC. Sequencing was performed by the SNP&SEQ Technology Platform in Uppsala. The facility is part of the National Genomics Infrastructure (NGI) Sweden and Science for Life Laboratory. The SNP&SEQ Platform is also supported by the Swedish Research Council and the Knut and Alice Wallenberg Foundation.

Supplementary materials

Supplementary material associated with this article can be found, in the online version, at doi:10.1016/j.watres.2023.120181.

References

Abe, K., Ueki, A., Ohtaki, Y., Kaku, N., Watanabe, K., Ueki, K., 2013. Anaerocella delicata gen. nov., sp. nov., a strictly anaerobic bacterium in the phylum Bacteroidetes isolated from a methanogenic reactor of cattle farms. J. Gen. Appl. Microbiol. 58, 405–412. https://doi.org/10.2323/jgam.58.405.

Ahmed, A.S., Bahreini, G., Ho, D., Sridhar, G., Gupta, M., Wessels, C., Marcelis, P., Elbeshbishy, E., Rosso, D., Santoro, D., Nakhla, G., 2019. Fate of cellulose in primary and secondary treatment at municipal water resource recovery facilities. Water Environ. Res. 91, 1479–1489. https://doi.org/10.1002/wer.1145.

Ali, M., Wang, Z., Salam, K.W., Hari, A.R., Pronk, M., van Loosdrecht, M.C.M., Saikaly, P. E., 2019. Importance of species sorting and immigration on the bacterial assembly of different-sized aggregates in a full-scale aerobic granular sludge plant. Environ. Sci. Technol. 53, 8291–8301. https://doi.org/10.1021/acs.est.8b07303.

Andreasen, K., Petersen, G., Thomsen, H., Strube, R., 1997. Reduction of nutrient emission by sludge hydrolysis. Water Sci. Technol. 35, 79–85. https://doi.org/10.1016/S0273-1223(97)00215-1.

Atasoy, M., Owusu-Agyeman, I., Plaza, E., Cetecioglu, Z., 2018. Bio-based volatile fatty acid production and recovery from waste streams: current status and future challenges. Bioresour. Technol. 268, 773–786. https://doi.org/10.1016/j.biortech.2018.07.042.

Bahreini, G., Elbahrawi, M., Elbeshbishy, E., Santoro, D., Nakhla, G., 2021. Biological nutrient removal enhancement using fermented primary and rotating belt filter biosolids. Sci. Total Environ. 796, 148947 https://doi.org/10.1016/j.scitotenv.2021.148947. –148947.

Bahreini, G., Elbeshbishy, E., Jimenez, J., Santoro, D., Nakhla, G., 2020a. Integrated fermentation and anaerobic digestion of primary sludges for simultaneous resource and energy recovery: impact of volatile fatty acids recovery. Waste Manag. 118, 341–349. https://doi.org/10.1016/j.wasman.2020.08.051.

Bahreini, G., Nazari, L., Ho, D., Flannery, C.C., Elbeshbishy, E., Santoro, D., Nakhla, G., 2020b. Enzymatic pre-treatment for enhancement of primary sludge fermentation. Bioresour. Technol. 305, 123071 https://doi.org/10.1016/j.biortech.2020.123071.

Banister, S.S., Pretorius, W.A., 1998. Optimisation of primary sludge acidogenic fermentation for biological nutrient removal. Water SA 24, 35–41.

Bouzas, A., Gabaldón, C., Marzal, P., Penya-Roja, J.M., Seco, A., 2002. Fermentation of municipal primary sludge: effect of SRT and solids concentration on volatile fatty acid production. Environ. Technol. (United Kingdom) 23, 863–875. https://doi.org/10.1080/09593332308618359.

Brison, A., Rossi, P., Gelb, A., Derlon, N., 2022. The capture technology matters: composition of municipal wastewater solids drives complexity of microbial community structure and volatile fatty acid profile during anaerobic fermentation. Sci. Total Environ. 815, 152762 https://doi.org/10.1016/j.scitotenv.2021.152762.

Callahan, B.J., McMurdie, P.J., Rosen, M.J., Han, A.W., Johnson, A.J.A., Holmes, S.P., 2016. DADA2: high-resolution sample inference from Illumina amplicon data. Nat. Methods 13, 581–583. https://doi.org/10.1038/nmeth.3869.

Chase, J.M., Kraft, N.J.B., Smith, K.G., Vellend, M., Inouye, B.D., 2011. Using null models to disentangle variation in community dissimilarity from variation in α-diversity. Ecosphere 2 (2). https://doi.org/10.1890/ES10-00117.1. Article 24.

Chase, J.M., Myers, J.A., 2011. Disentangling the importance of ecological niches from stochastic processes across scales. Philos. Trans. R. Soc. B Biol. Sci. 366, 2351–2363. https://doi.org/10.1098/rstb.2011.0063.

Chiu, Y.C., Chung, M.S., 2003. Determination of optimal COD/nitrate ratio for biological denitrification. Int. Biodeterior. Biodegrad. 51, 43–49. https://doi.org/10.1016/S0964-8305(02)00074-4.

Christensen, M.L., Jakobsen, A.H., Hansen, C.S.K., Skovbjerg, M., Andersen, R.B.M., Jensen, M.D., Sundmark, K., 2022. Pilot-scale hydrolysis of primary sludge for production of easily degradable carbon to treat biological wastewater or produce biogas. Sci. Total Environ. 846, 157532 https://doi.org/10.1016/j.scitotenv.2022.157532.

Cokgor, E.U., Oktay, S., Tas, D.O., Zengin, G.E., Orhon, D., 2009. Influence of pH and temperature on soluble substrate generation with primary sludge fermentation. Bioresour. Technol. 100, 380–386. https://doi.org/10.1016/j.biortech.2008.05.025.

Conca, V., da Ros, C., Valentino, F., Eusebi, A.L., Frison, N., Fatone, F., 2020. Long-term validation of polyhydroxyalkanoates production potential from the sidestream of municipal wastewater treatment plant at pilot scale. Chem. Eng. J. 390, 124627 https://doi.org/10.1016/j.cej.2020.124627.

Crutchik, D., Frison, N., Eusebi, A.L., Fatone, F., 2018. Biorefinery of cellulosic primary sludge towards targeted Short Chain Fatty Acids, phosphorus and methane recovery. Water Res. 136, 112–119. https://doi.org/10.1016/j.watres.2018.02.047.

Da Ros, C., Conca, V., Eusebi, A.L., Frison, N., Fatone, F., 2020. Sieving of municipal wastewater and recovery of bio-based volatile fatty acids at pilot scale. Water Res. 174, 115633 https://doi.org/10.1016/j.watres.2020.115633.

Dauknys, R., Haluza, A., Mažeikienė, A., 2019. Laboratory research of hydrolysis-acidogenesis process of primary sludge. J. Environ. Eng. 145, 1–6. https://doi.org/10.1061/(asce)ee.1943-7870.0001600.

de Celis, M., Duque, J., Marquina, D., Salvadó, H., Serrano, S., Arregui, L., Santos, A., Belda, I., 2022. Niche differentiation drives microbial community assembly and succession in full-scale activated sludge bioreactors. npj Biofilms Microbiomes 8, 1–6. https://doi.org/10.1038/s41522-022-00291-2.

Dueholm, M.K.D., Nierychlo, M., Andersen, K.S., Rudkjøbing, V., Knutsson, S., Global Consortium, M.I.D.A.S., Albertsen, M., Nielsen, P.H., 2022. MiDAS 4: a global catalogue of full-length 16S rRNA gene sequences and taxonomy for studies of bacterial communities in wastewater treatment plants. Nat. Commun. 13, 1–15. https://doi.org/10.1038/s41467-022-29438-7.

Eastman, J.A., Ferguson, J.F., 1981. Solubilization of particulate organic carbon during the acid phase of anaerobic digestion. J. Water Pollut. Control Fed. 53, 352–366.

Edgar, R.C., 2016. SINTAX: a simple non-Bayesian taxonomy classifier for 16S and ITS sequences. bioRxiv 74161. 10.1101/074161.
Ekholm, J., Persson, F., de Blois, M., Modin, O., Pronk, M., van Loosdrecht, M.C.M., Suarez, C., Gustavsson, D.J.I., Wilén, B.M., 2022. Full-scale aerobic granular sludge for municipal wastewater treatment - granule formation, microbial succession, and process performance. Environ. Sci. Water Res. Technol. 8, 3138–3154. https://doi.org/10.1039/d2ew00653g.
Elefsiniotis, P., Wareham, D.G., 2007. Utilization patterns of volatile fatty acids in the denitrification reaction. Enzyme Microb. Technol. 41, 92–97. https://doi.org/10.1016/j.enzmictec.2006.12.006.
Esquivel-Elizondo, S., Ilhan, Z.E., Garcia-Peña, E.I., Krajmalnik-Brown, R., 2017. Insights into butyrate production in a controlled fermentation system via gene predictions. mSystems 2. https://doi.org/10.1128/msystems.00051-17 e00051-17.
Ferreiro, N., Soto, M., 2003. Anaerobic hydrolysis of primary sludge: influence of sludge concentration and temperature. Water Sci. Technol. 47, 239–246. https://doi.org/10.2166/wst.2003.0652.
Ghasimi, D.S.M., de Kreuk, M., Maeng, S.K., Zandvoort, M.H., van Lier, J.B., 2016. High-rate thermophilic bio-methanation of the fine sieved fraction from Dutch municipal raw sewage: cost-effective potentials for on-site energy recovery. Appl. Energy 165, 569–582. https://doi.org/10.1016/j.apenergy.2015.12.065.
Ghasimi, D.S.M., Tao, Y., de Kreuk, M., Abbas, B., Zandvoort, M.H., van Lier, J.B., 2015. Digester performance and microbial community changes in thermophilic and mesophilic sequencing batch reactors fed with the fine sieved fraction of municipal sewage. Water Res 87, 483–493. https://doi.org/10.1016/j.watres.2015.04.027.
Griffin, J.S., Wells, G.F., 2017. Regional synchrony in full-scale activated sludge bioreactors due to deterministic microbial community assembly. ISME J. 11, 500–511. https://doi.org/10.1038/ismej.2016.121.
Hey, T., Jönsson, K., La Cour Jansen, J., 2012. Full-scale in-line hydrolysis and simulation for potential energy and resource savings in activated sludge - a case study. Environ. Technol. 33, 1819–1825. https://doi.org/10.1080/09593330.2011.650217.
Huang, X., Duan, C., Yu, J., Dong, W., Wang, H., 2021. Response of VFAs and microbial interspecific interaction to primary sludge fermentation temperature. J. Clean. Prod. 322, 129081 https://doi.org/10.1016/j.jclepro.2021.129081.
Ibrahim, V., Hey, T., Jönsson, K., 2014. Determining short chain fatty acids in sewage sludge hydrolysate: a comparison of three analytical methods and investigation of sample storage effects. J. Environ. Sci. 26, 926–933. https://doi.org/10.1016/S1001-0742(13)60516-1.
Könönen, E., Song, Y., Rautio, M., Finegold, S.M., et al., 2010. Alistipes. In: Krieg, N.R., Staley, J.T., Brown, D.R., Hedlund, B.P., Paster, B., Ward, N.L., et al. (Eds.), Bergey's Manual of Systematic Bacteriology, pp. 56–61. Vol 4.
Krieg, N.R., et al., 2010. Family V. Prevotellaceae fam. nov. In: Krieg, N.R., Staley, J.T., Brown, D.R., Hedlund, B.P., Paster, B., Ward, N.L., et al. (Eds.), Bergey's Manual of Systematic Bacteriology. Springer, pp. 85–102. Vol 4.
Lee, W.S., Chua, A.S.M., Yeoh, H.K., Ngoh, G.C., 2014. A review of the production and applications of waste-derived volatile fatty acids. Chem. Eng. J. 235, 83–99. https://doi.org/10.1016/j.cej.2013.09.002.
Liébana, R., Modin, O., Persson, F., Szabó, E., Hermansson, M., Wilén, B.M., 2019. Combined deterministic and stochastic processes control microbial succession in replicate granular biofilm reactors. Environ. Sci. Technol. 53, 4912–4921. https://doi.org/10.1021/acs.est.8b06669.
Lin, L., Li, X.yan, 2018. Acidogenic fermentation of iron-enhanced primary sedimentation sludge under different pH conditions for production of volatile fatty acids. Chemosphere 194, 692–700. https://doi.org/10.1016/j.chemosphere.2017.12.024.
Maspolim, Y., Zhou, Y., Guo, C., Xiao, K., Ng, W.J., 2015. The effect of pH on solubilization of organic matter and microbial community structures in sludge fermentation. Bioresour. Technol. 190, 289–298. https://doi.org/10.1016/j.biortech.2015.04.087.
Mei, R., Narihiro, T., Nobu, M.K., Kuroda, K., Liu, W.T., 2016. Evaluating digestion efficiency in full-scale anaerobic digesters by identifying active microbial populations through the lens of microbial activity. Sci. Rep. 26, 34090.
Miron, Y., Zeeman, G., Van Lier, J.B., Lettinga, G., 2000. The role of sludge retention time in the hydrolysis and acidification of lipids, carbohydrates and proteins during digestion of primary sludge in CSTR systems. Water Res. 34, 1705–1713. https://doi.org/10.1016/S0043-1354(99)00280-8.
Modin, O., Liébana, R., Saheb-Alam, S., Wilén, B.M., Suarez, C., Hermansson, M., Persson, F., 2020. Hill-based dissimilarity indices and null models for analysis of microbial community assembly. Microbiome 8, 132. https://doi.org/10.1186/s40168-020-00942-6.
Moser-Engeler, R., Udert, K.M., Wild, D., Siegrist, H., 1998. Products from primary sludge fermentation and their suitability for nutrient removal. Water Sci. Technol. 38, 265–273. https://doi.org/10.1016/S0273-1223(98)00411-9.
Oksanen, J., Simpson, G.L., Blanchet, F.G., Kindt, R., Legendre, P., Minchin, P.R., O'Hara, R.B., Solymos, P., Stevens, M.H.H., Szoecs, E., Wagner, H., Barbour, M., Bedward, M., Bolker, B., Borcard, D., Carvalho, G., Chirico, M., Caceres, M.D., Durand, S., Evangelista, H.B.A., FitzJohn, R., Friendly, M., Furneaux, B., Hannigan, G., Hill, M.O., Lahti, L., McGlinn, D., Ouellette, M.-.H., Cunha, E.R., Smith, T., Stier, A., Braak, C.J.F.T., Weedon, J., 2022. vegan: Community Ecology Package.
Pitman, A.R., Lotter, L.H., Alexander, W.V., Deacon, S.L., 1992. Fermentation of raw sludge and elutriation of resultant fatty acids to promote excess biological phosphorus removal. Water Sci. Technol. 25, 185–194. https://doi.org/10.2166/wst.1992.0494.
Precup, G., Vodnar, D.C., 2019. Gut Prevotella as a possible biomarker of diet and its eubiotic versus dysbiotic roles: a comprehensive literature review. Br. J. Nutr. 122, 131–140. https://doi.org/10.1017/S0007114519000680.
Ramsay, I.R., Pullammanappallil, P.C., 2001. Protein degradation during anaerobic wastewater treatment: derivation of stoichiometry. Biodegradation 12, 247–256. https://doi.org/10.1023/A:1013116728817.
Raup, D.M., Crick, R.E., 1979. Measurement of faunal similarity in paleontology. J. Paleontol. 53, 1213–1227.
Rieger, L., Gillot, S., Langergraber, G., Ohtsuki, T., Shaw, A., Takács, I., Winkler, S., 2013. Guidelines for Using Activated Sludge Models, Water Intelligence Online. IWA Publishing. https://doi.org/10.2166/9781780401164.
Rognes, T., Flouri, T., Nichols, B., Quince, C., Mahé, F., 2016. VSEARCH: a versatile open source tool for metagenomics. PeerJ 4, e2584. https://doi.org/10.7717/peerj.2584, 1–22.
Rusten, B., Rathnaweera, S.S., Rismyhr, E., Sahu, A.K., Ntiako, J., 2017. Rotating belt sieves for primary treatment, chemically enhanced primary treatment and secondary solids separation. Water Sci. Technol. 75, 2598–2606. https://doi.org/10.2166/wst.2017.145.
Skalsky, D.S., Daigger, G.T., 1995. Wastewater solids fermentation for volatile acid production and enhanced biological phosphorus removal. Water Environ. Res. 67, 230–237. https://doi.org/10.2175/106143095x131402.
Tykesson, E., Jönsson, L.E., la Cour Jansen, J., 2005. Experience from 10 years of full-scale operation with enhanced biological phosphorus removal at Öresundsverket. Water Sci. Technol. 52, 151–159. https://doi.org/10.2166/wst.2005.0451.
Ucisik, A.S., Henze, M., 2008. Biological hydrolysis and acidification of sludge under anaerobic conditions: the effect of sludge type and origin on the production and composition of volatile fatty acids. Water Res. 42, 3729–3738. https://doi.org/10.1016/j.watres.2008.06.010.
Väänänen, J., Cimbritz, M., La Cour Jansen, J., 2016. Microsieving in primary treatment: effect of chemical dosing. Water Sci. Technol. 74, 438–447. https://doi.org/10.2166/wst.2016.223.
van Lier, J.B., Nidal, M., Zeeman, G., 2020. Anaerobic wastewater treatment. In: Chen, G., van Loosdrecht, M.C.M., Ekama, G.A., Brdjanovic, D. (Eds.), Biological Wastewater Treatment: Principles, Modeling and Design. IWA Publishing, pp. 701–756.
Vanwonterghem, I., Jensen, P.D., Dennis, P.G., Hugenholtz, P., Rabaey, K., Tyson, G.W., 2014. Deterministic processes guide long-term synchronised population dynamics in replicate anaerobic digesters. ISME J 8, 2015–2028. https://doi.org/10.1038/ismej.2014.50.
Volke, E.I.P., Solon, K., Comeau, Y., Henze, M., 2020. Wastewater characteristics. In: Chen, G., van Loosdrecht, M.C.M., Ekama, G.A., Brdjanovic, D. (Eds.), Biological Wastewater Treatment: Principles, Modeling and Design. IWA Publishing, pp. 77–110.
Wang, X., Jin, P., Zhang, A., Gao, J., Zhang, B., Hou, Y., 2020. Effect of mechanical elutriation on carbon source recovery from primary sludge in a novel activated primary tank. Chemosphere 240, 124820. https://doi.org/10.1016/j.chemosphere.2019.124820.
Yuan, Y., Liu, Y., Li, B., Wang, B., Wang, S., Peng, Y., 2016. Short-chain fatty acids production and microbial community in sludge alkaline fermentation: long-term effect of temperature. Bioresour. Technol. 211, 685–690. https://doi.org/10.1016/j.biortech.2016.03.138.
Zhou, J., 2017. Stochastic community assembly : does it matter in microbial ecology? Microbiol. Mol. Biol. Rev. 81, 1–32.